https://doi.org/10.5194/egusphere-2026-2947
Preprint. Discussion started: 12 June 2026

Stoichiometric deviation and regulatory mechanisms of AOU-nutrient ratio in the oligotrophic Northwest Pacific Ocean

Detong Tian[1], Xuegang Li[2,3*], Jinming Song[2,3], Yunping Xu[1], Feng Zhao[2], Jun Ma[2,3], Shanshan Liu[2,3], Muhammad Inayat Ullah Khan[1], Weichao Wu[1,4*]

[1]College of Oceanography and Ecological Science, Shanghai Ocean University, Shanghai, 201306, China

[2]Institute of Oceanology, Chinese Academy of Sciences, Qingdao 266000, China

[3]Laboratory for Marine Ecology and Environmental Science, Qingdao Marine Science and Technology Center, Qingdao 266237, China

[4]International Research Center for Marine Biosciences at Shanghai Ocean University, Ministry of Science and Technology, China

*Correspondence: W. Wu (wcwu@shou.edu.cn) and X. Li (lixuegang@qdio.ac.cn)

Abstract

In oligotrophic oceans, the stoichiometric ratios of apparent oxygen utilization (AOU) to nutrients often deviate from the classical Redfield ratio, yet the mechanisms driving these deviations remain poorly constrained. Contrary to the commonly held view that ratios of AOU to nutrients are typically elevated, our study found that the mean ratios of AOU to dissolved inorganic nitrogen (DIN) and AOU to dissolved inorganic phosphorus (DIP) in the upper 2000 m of the oligotrophic Northwest Pacific are substantially lower than the classical Redfield ratios (8.6 and 138, respectively), measuring only 6.28 and 86.79, respectively. Physical mixing alone cannot explain these low ratios, as the region is strongly stratified. This persistent vertical isolation drives chronic nutrient limitation in surface waters, promoting phytoplankton to produce carbon-rich transparent exopolymer particles (TEPs) with high C:N ratios. Meanwhile, the microbial community, dominated by *Pelagibacter* and *Alteromonas*, exhibits functional partitioning. *Pelagibacter* efficiently recycles small organic molecules, while *Alteromonas* degrades complex polymers and actively releases

https://doi.org/10.5194/egusphere-2026-2947
Preprint. Discussion started: 12 June 2026

phosphate. This selective processing enhances nutrient regeneration relative to carbon oxidation, depressing the AOU/nutrient ratios. These findings suggest that biogeochemical models should account for such biological feedbacks to improve predictions of ocean carbon export and nutrient cycling under future climate scenarios.

1. Introduction

The ocean is the largest active reservoir of carbon and nutrients on Earth, and its internal biogeochemical cycles are crucial for sustaining the productivity of marine ecosystems (Friedlingstein et al., 2025). The supply of nutrients such as nitrogen and phosphorus directly affects marine primary productivity, and the regeneration of these nutrients is closely coupled with the production, export, and burial of organic carbon, thereby collectively regulating the intensity of the marine biological pump and the global carbon cycle (Longhurst and Glen Harrison, 1989; Smith et al., 2008). Apparent oxygen utilization (AOU) serves as a key link between surface photosynthesis and deep-water heterotrophic respiration and reflects the amount of dissolved oxygen (DO) consumed by respiration during the transport and sedimentation of organic matter in water masses (Ito et al., 2004; Sulpis et al., 2023). Classical Redfield stoichiometry establishes a proportional relationship between AOU, nutrient regeneration, and the accumulation of dissolved inorganic carbon (DIC), which has led to the widespread use of AOU/nutrient ratios, such as AOU/dissolved inorganic nitrogen (DIN) and AOU/dissolved inorganic phosphorus (DIP) ratios, to infer the elemental composition of degraded organic matter (Tanioka and Matsumoto, 2020). However, the relationships between AOU and nutrients in marine environments often deviate from classical stoichiometry, highlighting the presence of complex physical and biogeochemical regulatory mechanisms.

Numerous observations indicate that the AOU/nutrient ratios in many oceanic regions generally exceed the classical Redfield ratio (i.e., AOU/DIN = 8.6 and AOU/DIP = 138) (Anderson and Sarmiento, 1994; Delaigue et al., 2024). This pattern is particularly evident in highly stratified oligotrophic waters, where the degradation rates of suspended and dissolved organic matter are slow, and spatiotemporal

https://doi.org/10.5194/egusphere-2026-2947
Preprint. Discussion started: 12 June 2026

decoupling between production and remineralization occurs (Dai et al., 2023). In these areas, some organic matter may migrate horizontally before settling or undergo multiple cycles within surface waters. Simultaneously, the C:N ratio of nitrogen sources supplied by nitrogen-fixing organisms is generally higher than the Redfield value, resulting in greater oxygen consumption per unit of nitrogen regenerated during degradation (Körtzinger et al., 2001; Singh et al., 2015). Furthermore, DIC generated by shallow respiration as a result of organic matter degradation by heterotrophic organisms may precede nutrient regeneration, and potential non-photosynthetic oxidation processes also contribute to elevated AOU/nutrient ratios in oligotrophic regions (Calleja et al., 2019). In contrast, in well-mixed marginal shelf seas where organic matter sources are complex, strong physical agitation disrupts the coupling between AOU and nutrients. This leads to highly scattered ratios that are systematically lower than the Redfield values, reflecting the influence of physical processes on biogeochemical signals (Zhu et al., 2025). To distinguish physical from biological influences, chemical tracers such as preformed nitrate ($PreNO_3$) and preformed phosphate ($PrePO_4$) are widely used, as they effectively separate nutrients pre-existing in water masses from those regenerated locally (Letscher and Villareal, 2018). Applying such tracers to strongly stratified oligotrophic oceans, where physical mixing is weak, facilitates the isolation of biogeochemical signals, thereby revealing the dominant role of internal processes in shaping the observed AOU-nutrient relationships.

The Tropical Northwest Pacific (TNWP) is a key region for global ocean circulation and biogeochemical cycling, featuring the Western Pacific Warm Pool (WPWP), the world's largest warm-water body, where high sea surface temperatures and strong stratification create an extensive oligotrophic zone (Radenac et al., 2013). Complex ocean circulation systems converge here, forming vertically layered water masses that significantly influence nutrient supply, organic matter production, transport, and transformation (Hu, D et al., 2015; Jian et al., 2022; Sun, C et al., 2008). Numerous studies have characterized the macroscopic distribution of nutrients in this region (Ma et al., 2021a) as well as the vertical degradation patterns of particulate organic carbon

https://doi.org/10.5194/egusphere-2026-2947
Preprint. Discussion started: 12 June 2026

(POC) (Tian et al., 2025). However, POC is a complex mixture comprising components with diverse chemical compositions and sources, and its various components differ significantly in terms of bioavailability and their roles in the carbon cycle (Kharbush et al., 2020). Therefore, the roles of specific functional particulate components within POC in regional organic matter transport and transformation have gradually become a focus of research in recent years (Digernes et al., 2025). Among these components, transparent exopolymer particles (TEPs) is a class of polysaccharide colloid primarily secreted by phytoplankton, characterized by a high C:N ratio (Engel and Passow, 2001). They accumulate in large quantities in oligotrophic surface waters and may alter the kinetics and degradation pathways of particulate matter (Kodama et al., 2014). Meanwhile, regional differences in microbial community structure and function are considered to directly affect organic matter degradation and nutrient regeneration processes, thereby regulating the stoichiometry of deep nutrient regeneration and efficiency of the carbon cycle (Guo et al., 2023; Saavedra et al., 2025). However, although numerous studies have revealed several biogeochemical characteristics of this region from different perspectives, our overall understanding remains relatively fragmented. In particular, the stoichiometric characteristics of organic matter degradation in water masses of varying sources and ages, as well as the mechanisms driving deviations from the Redfield ratios, remain unclear. Additionally, there is a lack of systematic field evidence regarding how microbial metabolic strategies influence the coupled cycles of carbon, nitrogen, and phosphorus.

In the present study, suspended particulate organic matter (POM) and water samples were collected from six water columns within and around the core area of the TNWP Warm Pool. The aim was to elucidate the coupled mechanism linking physical stratification, organic matter transformation, nutrient regeneration, and microbial regulation in the oligotrophic waters of the western Pacific by integrating multiple biogeochemical and microbial parameters across distinct water masses.

2. Materials and Methods

2.1 Research area and sample collection:

https://doi.org/10.5194/egusphere-2026-2947
Preprint. Discussion started: 12 June 2026

From February to April 2022, a research cruise was conducted aboard the R/V *Kexue* (voyage NORC2021-09) in the TNWP Warm Pool. During the survey, a total of six sampling stations were set up: EQ-6, E142-3, E142-7, E142-11, E142-13, and E142-19 (Fig. 1).

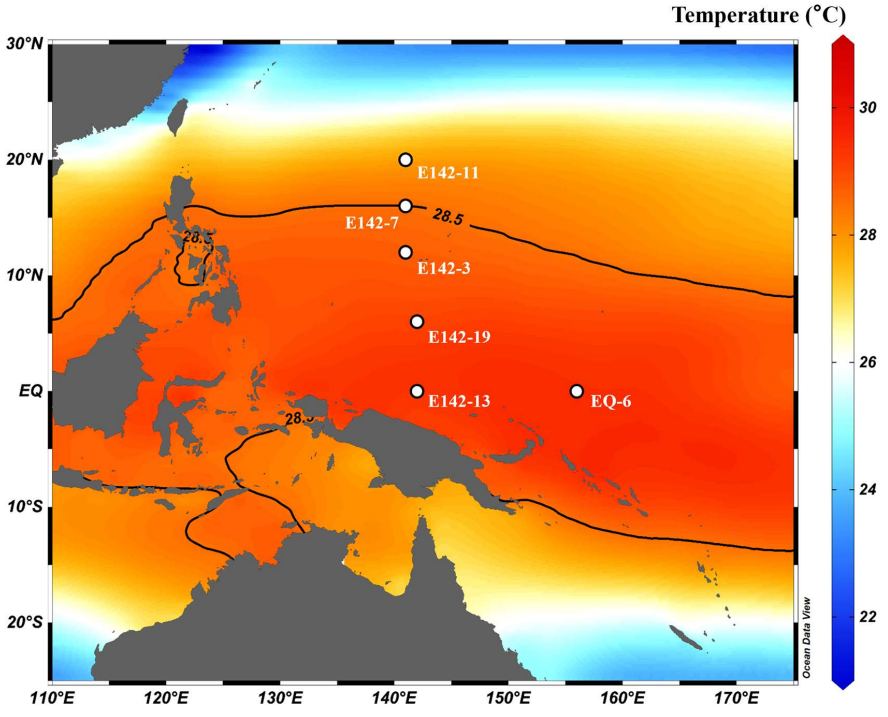

Figure 1. Study area and sampling stations in the Tropical Northwest Pacific. The sampling area is located in the Western Pacific Warm Pool, and the 28.5 °C isotherms are shown as black lines.

Seawater samples were collected from 16 depths (5, 50, 100, 150, 200, 300, 400, 500, 600, 800, 1,000, 1,200, 1,400, 1,600, 1,800, and 2,000 m) using 12 L Niskin bottles (KC-Denmark, Denmark) mounted on a shipboard CTD rosette (Conductivity-Temperature-Depth, Sea-bird SBE911, United States). After seawater collection, DO samples were first aliquoted and fixed in 50 mL amber glass bottles. Then, the seawater was filtered through pre-combusted and acid-washed GF/F glass fiber filters (0.7 μm pore size, Whatman; 450 °C for 4 h, 0.5 M HCl for 24 h), followed by the collection of

https://doi.org/10.5194/egusphere-2026-2947
Preprint. Discussion started: 12 June 2026

nutrient and DIC samples. Samples for nutrient determination were aliquoted into 250 mL high-density polyethylene bottles, fixed with chloroform, and stored at -20°C before measurement. Samples for DIC analysis were collected in 50 mL airtight glass bottles. After overflow, 1 mL of the water sample was withdrawn and the remaining sample was poisoned with saturated mercuric chloride solution to suppress biological activity. The samples were stored at 4°C until analysis.

Suspended particulate samples for POC analysis were collected by filtering 2−4 L of seawater through pre-combusted and acid-washed GF/F glass fiber filters (0.7 µm pore size, Whatman; 450 °C for 4 h, 0.5 M HCl for 24 h). Samples were stored at -20 °C until measurement. TEP samples were collected by filtering 1−4 L of seawater through polycarbonate filters (0.45 µm pore size, Whatman) under a vacuum of < 170 mmHg. The filtered membrane was stained with 0.5−1 mL of a 400 mg L^{-1} Alcian Blue solution (Sigma-Aldrich, USA) for 5−10 s, rinsed with 5 mL of MilliQ water, and stored at -20 °C until measurement (three replicate samples were collected at each depth). Samples for chlorophyll-a (Chl-*a*) determination were collected from five depths between 5 and 200 m. First, 2 L of seawater samples were filtered through a 200 µm mesh to remove zooplankton and then filtered onto a 0.7 µm GF/F glass fiber membrane (Whatman; 450 °C for 4 h, 0.5 M HCl for 24 h). The filters were then stored at -20 °C until analysis in the shore-based laboratory. Seawater samples (20 L) for microbial community analysis were similarly pre-filtered through a 200 µm mesh and then filtered through a 0.22 µm mixed cellulose ester (MCE) membrane. The filtered samples were immediately transferred to cryovials, supplemented with RNA Later stabiliser (Qiagen, Germany), and stored at -80 °C.

2.2. Chemical analysis

2.2.1 Temperature, salinity, DO, and Chl-*a*

For each station, temperature, salinity, and DO were measured in situ using a shipboard CTD. Simultaneously, discrete DO samples were fixed and titrated according to the Winkler method with an accuracy of 0.22 µmol L^{-1} (Bryan et al., 1976). These

https://doi.org/10.5194/egusphere-2026-2947
Preprint. Discussion started: 12 June 2026

discrete DO samples were used to calibrate the DO concentration data obtained from the CTD sensor. Chl-*a* concentrations were determined by acetone extraction. Filters containing Chl-*a* were extracted with 90 % acetone for 14 h, and the Chl-*a* concentration was then measured using a Turner fluorometer (Turner Designs, United States) (Ma et al., 2020).

2.2.2 Nutrients

Phosphate (PO_4-P, as dissolved inorganic phosphorus, DIP), nitrate (NO_3-N), nitrite (NO_2-N), ammonium (NH_4-N), and silicate (SiO_3-Si, as dissolved inorganic silicon, DSi) concentrations were determined using a QuAAtro nutrient analyzer (SEAL, Germany). The limits of detection for PO_4-P, NO_3-N, NO_2-N, and NH_4-N were 0.01, 0.02, 0.01, 0.01 and 0.01 μmol L^{-1}, respectively (Ma et al., 2020). The DIN concentration was the sum of the concentrations of NO_3-N, NO_2-N, and NH_4-N.

2.2.3 POC and DIC

The particulate filters were freeze-dried at -50 °C for 24 h. After drying, the filters were acid-fumed with concentrated hydrochloric acid for 12 h to remove inorganic carbonates and then dried at < 60 °C. The dried membrane samples were wrapped in a tin boat for subsequent analysis. The pretreated samples were analyzed for POC concentration using an elemental analyzer (Thermo Fisher Scientific Flash EA 1112, United States), with an analytical precision of ± 0.8‰. POC measurements were calibrated using standard reference materials, including USGS64 (C % = 31.97 %, Indiana University), USGS40 (C % = 40.8 %, U.S. Geological Survey), and Urea #2a (C % = 20 %, Indiana University) (Ma et al., 2021b).

DIC concentrations were determined using an Apollo SciTech AS-C3 analyzer (United States) with an analytical precision of ±0.1 % (Ma et al., 2020). Calibration was performed using certified reference material (batch 144, 2031.53 ± 0.62 μmol L^{-1}) provided by the Scripps Institution of Oceanography (University of California, San Diego).

2.2.4 TEP

https://doi.org/10.5194/egusphere-2026-2947
Preprint. Discussion started: 12 June 2026

In the shore-based laboratory, the TEP filters were transferred to a 10 mL amber glass bottle, and 6 mL of 80 % (14.4 M) sulfuric acid solution was added for 10 h with periodic gentle mixing. The absorbance was then measured at 787 nm using a spectrophotometer (UV-1600, Shimadzu). The absorbance was converted to xanthan gum equivalents (Xeq) weight using a calibration curve derived by Bittar et al. (2018), with a detection limit of approximately 5.6 µg Xeq L^{-1} (Bittar et al., 2018).

2.2.5 Relative abundance of microorganisms

DNA was extracted from the filters using the AllPrep DNA/RNA Mini Kit (Qiagen, Germany). 16S rDNA was amplified using a universal bacterial primer set, F515 (5'GTGCCAGCMGCCGCGG3') and R907 (5'CCGTCAATTCMTTTR AGTTT3'). To reduce PCR bias, three replicate PCR reactions were performed for each sample. The amplicon libraries were sequenced using the Illumina NovaSeq platform (Novogene, China). During data processing, primers and low-quality reads were removed using VSEARCH (v. 2.15.2), and sequences were denoised using USEARCH (v. 10.0.240) to obtain an amplicon sequence variant (ASV) table. The amplicon sequence variants (ASVs) were then analyzed using VSEARCH (v. 2.15.2) against a reference database. The RDP database (v. 16) was used to annotate the ASV tables. The ASV tables were standardized by resampling to ensure that the data from each sample are at the same level of comparison. The number of sequences assigned to each ASV in each sample was normalized to its proportion of total reads to calculate the relative abundance of microbial taxa (Liu et al., 2024).

2.3 Tracer computations

To account for the non-Redfield stoichiometric characteristics of dissolved organic matter (DOM), we applied an improved method for calculating residual $PreNO_3$ tracer (Letscher and Villareal, 2018):

$$\text{residual } PreNO_3 = NO_{3meas} - (f_{DOM} \bullet \frac{AOU}{r_{DOM}}) - (f_{POM} \bullet \frac{AOU}{r_{POM}}) \quad (1),$$

https://doi.org/10.5194/egusphere-2026-2947
Preprint. Discussion started: 12 June 2026

where measured nitrate (NO_{3meas}) is defined as the sum of the concentrations of NO_3-N and NO_2-N. AOU is given by:

$$AOU = DO_{sat} - DO_{meas} \quad (2),$$

where DO_{sat} is the saturated DO concentration at a given temperature, salinity, and pressure (Garcia and Gordon, 1992), and DO_{meas} is the measured DO concentration.

f_{DOM} and f_{POM} represent the fractions of total oxygen consumption attributed to DOM and POM, respectively. r_{DOM} and r_{POM} denote the stoichiometric ratios of O_2 consumed and regenerated nitrogen consumed during the remineralization of DOM and POM, respectively. The above parameters were selected based on water depth or neutral density (γ_n) of the water masses, following Letscher and Villareal (2018) (Table 1).

Similarly, the residual $PrePO_4$ tracer was computed as:

$$\text{residual } PrePO_4 = PO_{4meas} - (f_{DOM} \bullet \frac{AOU}{r_{DOM}}) - (f_{POM} \bullet \frac{AOU}{r_{POM}}) \quad (3),$$

We convert nitrogen-based stoichiometric coefficients to phosphorus equivalents using a DON:DOP ratio of 16:1, following the stoichiometry of semi-labile DOM in North Pacific (Letscher and Villareal, 2018).

Table 1. Parameters for the calculation of residual $PreNO_3$/$PrePO_4$ in the Pacific Ocean

Depth (m)/neutral density (γ_n)	f_{DOM}	f_{POM}	r_{POM}	r_{DOM}
0−100 m/γ_n: 24.2−24.7	0.5	0.5	6.9, 8.75, 10.6	18.1
γ_n> 24.7	0.5	0.5	6.9, 8.75, 10.6	18.9

2.4 Data Processing

Data processing was performed using OriginPro 2021 (v. 9.8.0.200). Depending on whether the variables follow a normal distribution, correlation analyses were performed using either Pearson's or Spearman's rho test (two-tailed, $\alpha = 0.05$), with $p < 0.05$ considered significant. The normality of the data was tested using the Kolmogorov-Smirnov test (two-tailed, $\alpha = 0.05$). The AOU/nutrient ratios were

https://doi.org/10.5194/egusphere-2026-2947
Preprint. Discussion started: 12 June 2026

10

estimated via simple linear regression using the ordinary least squares method, where AOU served as the independent variable and the nutrient (nitrate or dissolved inorganic phosphate) as the dependent variable. The slope of the resulting regression line represents the AOU per mole of nutrient regenerated (Álvarez-Salgado et al., 2014).

3. Results

3.1 Hydrological characteristics of the study area

Temperature-salinity (T-S) diagram and the vertical distribution of temperature, salinity, and γ_n indicate pronounced stratification in the water column, with eight distinct water masses identified (Fig. 2a, Table 2) (*Sun et al.,* 2008). γ_n increases with depth from approximately 21.6 to 27.7 kg m^{-3} (Fig. 2d), marking a clear transition from low-density tropical surface waters to high-density deep waters.

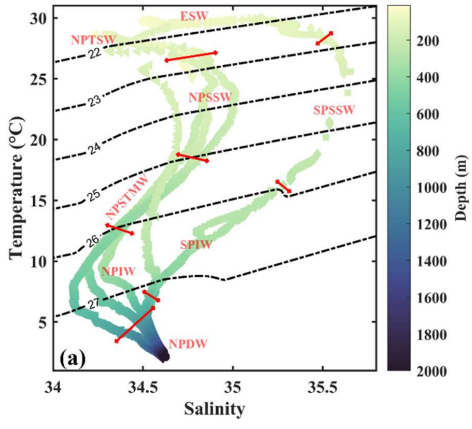

Table 2. Characteristics of water masses in the study area

Water Masses	Temperature (°C)	Salinity (‰)	γ_n (Kg m^{-3})
NPTSW	27.99-29.45 (28.71)	34.29-34.63 (34.45)	21.62-22.58 (21.76)
ESW	29.28-29.87 (29.56)	34.59-35.27 (35.01)	21.44-22.76 (21.89)
SPSSW	19.62-26.64 (22.95)	35.46-35.52 (35.51)	22.93-25.95 (24.25)
NPSSW	18.76-27.04 (23.89)	34.62-34.98 (34.80)	22.59-24.99 (23.51)
NPSTMW	13.23-16.45 (15.00)	34.42-34.68 (34.55)	25.00-26.00 (25.67)
NPIW	3.91-11.16 (7.36)	34.12-34.58 (34.40)	26.01-27.59 (26.99)
SPIW	5.47-12.43 (8.55)	34.52-34.94 (34.65)	26.00-27.40 (26.99)
NPDW	2.05-4.63 (3.07)	34.51-34.63 (34.58)	27.41-27.92 (27.76)

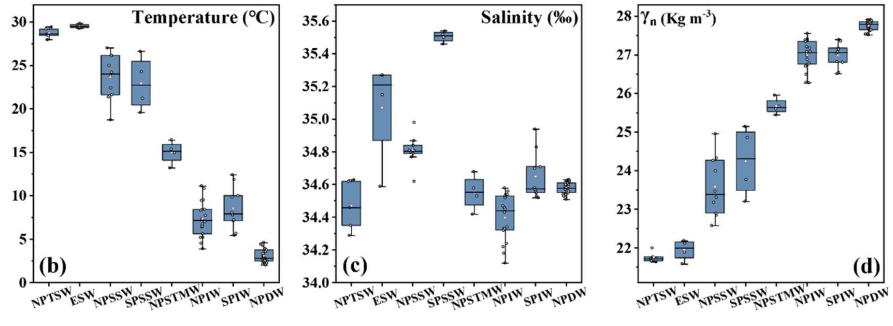

Figure 2. Physical properties of water masses in the research area. (a) Temperature-salinity diagram of six stations, and the distribution characteristics of (b) temperature,

https://doi.org/10.5194/egusphere-2026-2947
Preprint. Discussion started: 12 June 2026

(c) salinity, (d) neutral density of each water mass.

In the upper 200-meter water column, tropical surface waters and subsurface waters dominate. The North Pacific Tropical Surface Water (NPTSW) and Equatorial Surface Water (ESW) lie at the warmest end of the T-S diagram, with temperatures ranging from approximately 28−30 °C, characteristics of the WPWP. Below the mixed layer, the North Pacific Subsurface Water (NPSSW) and South Pacific Subsurface Water (SPSSW) exhibit pronounced salinity maxima along the 23−25 kg m^{-3} isopycnals. Both water masses have temperatures lower than the overlying surface waters (approximately 19−27 °C). The salinity of the SPSSW is the highest in the upper ocean (mean 35.51), while the NPSSW is slightly fresher (mean 34.80). These high-salinity tongue-like intrusions indicate active subduction and lateral transport processes within the thermocline. The North Pacific Subtropical Mode Water (NPSTMW) constitutes the transition layer between the thermocline and the intermediate waters, with physicochemical properties tightly constrained within a narrow range and demonstrating strong vertical homogeneity (Figs. 2b-d). Below approximately 300−400 m, the water column is dominated by intermediate waters originating from both hemispheres. The North Pacific Intermediate Water (NPIW) is characterized by low salinity (mean 34.12), exhibiting a salinity minimum in the T-S diagram (Fig. 2a). The South Pacific Intermediate Water (SPIW) has slightly higher temperature and salinity relative to NPIW. Its γ_n value largely overlaps with those of the NPIW, suggesting substantial mixing between the two within the study area. Below approximately 1000 m, the North Pacific Deep Water (NPDW) becomes predominant, exhibiting low temperatures, relatively uniform salinity, and high density. Its hydrographic properties cluster tightly in box plots, reflecting high stability (Figs. 2b-d). In summary, the water masses in the study area exhibit a precise vertical sequence: warm, low-density surface waters overlie a high-salinity thermocline/modal-water layer, which in turn overlies low-salinity intermediate waters and homogeneous deep waters. This stratified structure creates a vertically isolated physical regime that strongly suppresses vertical exchange of heat, dissolved constituents, and particulate matter.

https://doi.org/10.5194/egusphere-2026-2947
Preprint. Discussion started: 12 June 2026

3.2 Concentration and distribution of chemical parameters of each water mass

Nitrate, phosphate, and silicate concentrations were lowest in warm, low-density surface water masses (NPTSW, ESW) and gradually increased in the subsurface high-salinity water masses (SPSSW, NPSSW, NPSTMW). Local highs were reached in the intermediate water masses (NPIW, SPIW), indicating that these water masses are important reservoirs for regenerated nutrients. The deep water masses (NPDW) exhibited the highest nutrient concentrations, reflecting the accumulation of organic matter degradation products over long time scales (Figs. 3a-c). Calculations of $PreNO_3$ and $PrePO_4$ based on empirical relationships between DO and nutrients further resolve the proportions of nutrients supplied by physical transport versus local regeneration in each water mass (Figs. 3d, e). Both $PreNO_3$ and $PrePO_4$ increased from the surface to the intermediate and deep waters. Notably, $PrePO_4$ and $PreNO_3$ in surface waters should approach zero theoretically, yet positive anomalies were observed in NPTSW and ESW. With increasing depth, $PreNO_3$ and $PrePO_4$ concentrations in the intermediate waters increase and reach their maxima in the deep waters, where their spatial distributions are homogeneous, further indicating that this layer acts as an accumulation pool for long-term products of biogeochemical processes.

https://doi.org/10.5194/egusphere-2026-2947
Preprint. Discussion started: 12 June 2026

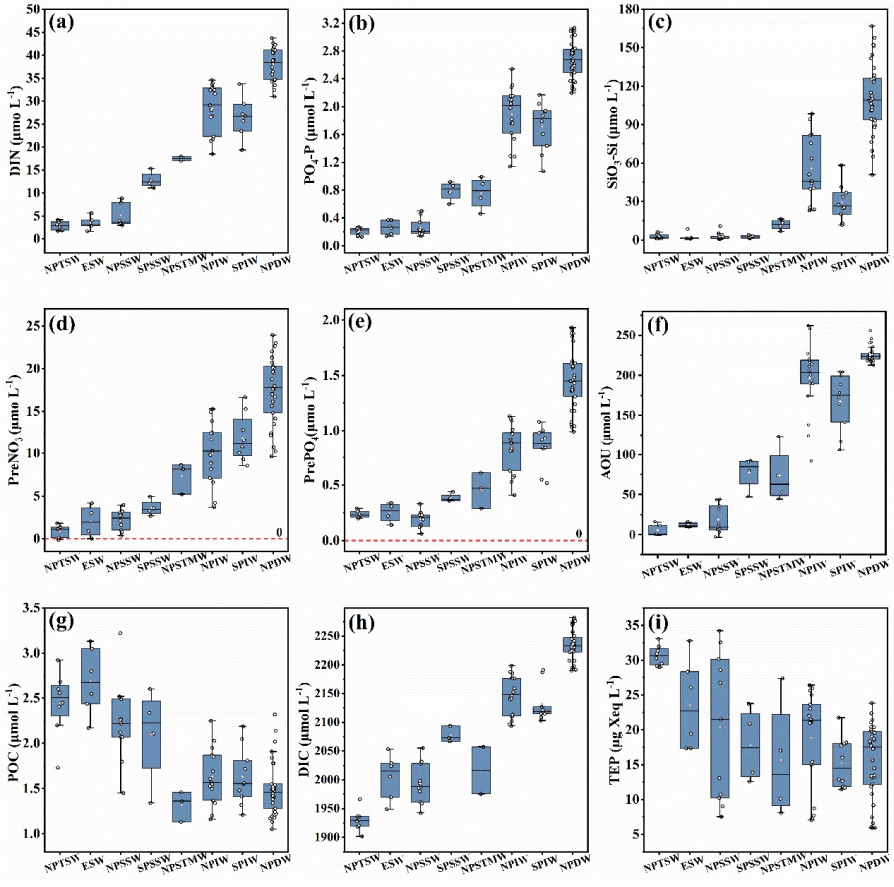

Figure 3. Distribution of (a) dissolved inorganic nitrogen (DIN), (b) phosphate (PO_4-P, as dissolved inorganic phosphorus, DIP), (c) silicate (SiO_3-Si, as dissolved inorganic silicon, DSi), (d) preformed nitrate ($PreNO_3$), (e) preformed phosphate ($PrePO_4$), (f) apparent oxygen utilization (AOU), (g) particulate organic carbon (POC), (h) dissolved inorganic carbon (DIC), (i) transparent exopolymer particle (TEP) at each water mass.

The vertical distribution pattern of DIC is consistent with that of nutrient regeneration: DIC concentrations are lowest in the surface waters, increase markedly from the subsurface and mode waters, and attain high values in the intermediate and deep waters (Fig. 3h). In contrast, POC and TEP exhibit a distribution pattern that is nearly opposite to that of nutrients and DIC among the different water masses. The surface and subsurface water masses contain higher POC and TEP contents, with TEP reaching a maximum of 34.22 μg Xeq L^{-1}, reflecting the aggregation of surface plankton

https://doi.org/10.5194/egusphere-2026-2947
Preprint. Discussion started: 12 June 2026

and bacterial extracellular secretions. POC concentrations decrease substantially in the intermediate and deep waters, while the AOU continuously increased, indicating that organic particles are transitioning from the production phase to the remineralization phase (Figs. 3f, g). In contrast, TEP concentrations decrease more slowly and remain within a measurable range even in the deep waters (Fig. 3i). The persistence of such polymers in the deep waters influences the composition of organic matter and modify pathways of carbon cycling.

3.3 Microbial community structure

Among the identified dominant genera, *Pelagibacter* and *Alteromonas* occur at relatively high proportions in all water masses, followed by *Nitrosopumilus*, whereas *Halomonas* and *Alcanivorax* remain minor taxa (Fig. 4). *Pelagibacter*, a typical oligotrophic bacterium, has a highly streamlined genome and is efficient in utilizing small organic molecules, enabling it to thrive in upper water column environments with low nutrient concentrations but relatively stable dissolved organic matter fluxes. Therefore, in both surface and subsurface water masses, *Pelagibacter* exhibits the highest relative abundance of 15 %–24 %. In these water masses, *Alteromonas* maintains a relatively stable relative abundance of 14 %−17 %, while *Nitrosopumilus* accounts for only 0−6 %, and *Halomonas* and *Alcanivorax* each contribute < 2 %. In the transitional water mass NPSTMW, the community structure undergoes significant reorganization. The proportion of *Pelagibacter* decreases to ~16 %, while *Alteromonas* increases to ~25 %, the highest among all water masses. *Nitrosopumilus* also rises to 13 %, and *Halomonas* increases to 4 %. This depth layer corresponds to the interface between water masses, where nutrients concentrations increase sharply and POC concentrations decrease markedly (Fig. 3f), and the microbial community shifts from being dominated by oligotrophic groups represented by *Pelagibacter* to a structure jointly dominated by opportunistic heterotrophic bacteria (e.g., *Alteromonas*) and chemoautotrophic ammonia-oxidizing archaea (e.g., *Nitrosopumilus*). In intermediate and deep water masses, the proportion of *Pelagibacter* further decreases to 3 %−6 %, while *Alteromonas* remains at a relatively high level of 14 %−23 %, and the proportions

https://doi.org/10.5194/egusphere-2026-2947
Preprint. Discussion started: 12 June 2026

of *Halomonas* and *Alcanivorax* also increase. The high relative abundance of *Alteromonas* suggests that regenerative biogeochemical processes, characterized by the decomposition of heterotrophic organic matter and the release of nutrients, dominate in these water masses. Meanwhile, the increase of *Halomonas* and *Alcanivorax* in intermediate and deep water masses reflects the adaptation of opportunistic bacteria to high-salinity and recalcitrant organic matter environments, suggesting that these taxa may contribute to the further transformation of deep organic carbon.

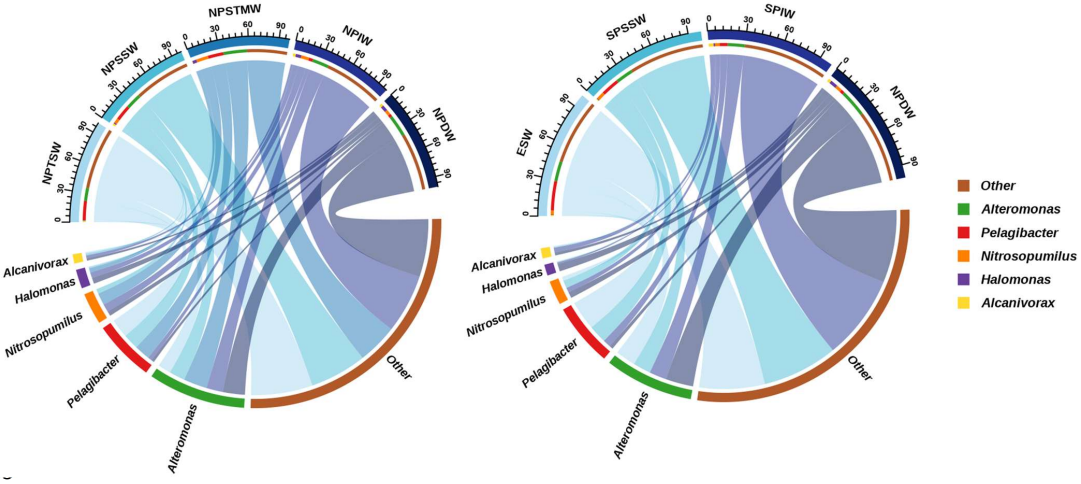

Figure 4. Relative abundance (%) and diversity of major microbial genera in each water mass

4. Discussion

4.1 Spatial variation and controlling factors of nutrient dynamics in TNWP water masses

The AOU of the ocean water column is an important indicator of the intensity of organic matter remineralization and oxygen consumption (*Sulpis et al.*, 2023). In the surface and subsurface water masses of the study area, AOU is slightly negative and close to zero, reflecting photosynthetic oxygen production and bubble injection (Fig. 3f). From the surface to the intermediate water mass, AOU increases rapidly, indicating intensified organic-matter remineralization dominated by heterotrophic respiration (Fig.

https://doi.org/10.5194/egusphere-2026-2947
Preprint. Discussion started: 12 June 2026

3f). In NPDW, AOU increases to a maximum of approximately 225 μmol L^{-1} and then remains relatively stable, suggesting a dynamic balance between oxygen consumption and supply (Fig. 5). In this study area, the AOU/DIN and AOU/DIP of the total water column are 6.28 and 86.79, respectively, much lower than the ideal Redfield model (i.e., AOU/DIN = 8.6, AOU/DIP = 138) (Redfield, 1960) and also lower than the reported values from the Atlantic and Indian Oceans (AOU/DIN = 10.6, AOU/DIP = 170) (Anderson and Sarmiento, 1994). Although previous studies have shown that in strongly mixed ocean areas, enhanced water aeration and shorter water mass residence time can systematically suppress linear regression slopes (AOU/DIN = 3.1, AOU/DIP = 57.6) (Zhu et al., 2025), our study area is located in the WPWP, where strong stratification inhibits vertical mixing and exchange (Hu, D et al., 2015). Hence, physical "noise" is weak, and the low ratios observed here are more likely to originate from biogeochemical processes operating within the water masses.

To examine how these biogeochemical processes vary across water masses, we calculated AOU/nutrient regression slopes separately for the upper (0−300 m), middle (300−1000 m), and deep (> 1000 m) water masses (Fig. 5). The AOU/DIN value is lowest in the upper water mass (6.87), increases in the middle water mass (7.21), and becomes statistically insignificant in the deep water mass ($p > 0.05$) (Fig. 5a). The AOU/DIP slopes follow a consistent pattern: lowest in the upper water mass (103.17), increasing in the middle water mass (116.04), and non-significant in the deep water mass (Fig. 5b). The low AOU/nutrients values in the upper water mass reflect a pronounced surplus of nitrogen and phosphorus relative to oxygen consumption. This surplus is driven by the synthesis of carbon-rich transparent exopolymer particles (TEP). Due to insufficient vertical mixing, surface nutrients are not replenished after consumption, resulting in persistently low concentrations (Figs. 3a-c) and strong oligotrophy (Chl-*a* in the deep chlorophyll maximum: 0.19−0.31 μg L^{-1}). Under this nutrient stress, phytoplankton synthesize TEP with a high C:N ratio (25−35) rather than investing in biomass (Yamada et al., 2017; Zamanillo et al., 2019), as evidenced by high TEP concentrations in surface and subsurface waters (Fig. 3i). TEP production sustains

https://doi.org/10.5194/egusphere-2026-2947
Preprint. Discussion started: 12 June 2026

oxygen evolution while consuming little nitrogen and phosphorus, generating positive $PreNO_3$/$PrePO_4$ anomalies (Figs. 3d, e) (Curran et al., 2025; Smyth and Letscher, 2023). In addition, since microorganisms preferentially degrade low-C:N substrates (e.g., proteins), the carbon-rich TEP is remineralized slowly, causing net nutrient regeneration to exceed organic carbon oxidation, thereby depressing the linear regression slopes of AOU/DIN and AOU/DIP in the study area (Figs. 5a, b) (Hwang et al., 2006; Tian et al., 2025). In the deep water mass, the absence of significant AOU/nutrients relationships is consistent with microbial processes that decouple oxygen consumption from nutrient regeneration, including chemoautotrophy mediated by ammonia-oxidizing archaea such as *Nitrosopumilus* (Martens-Habbena et al., 2009) and alternative phosphorus cycling via alkaline phosphatase activity of *Alteromonas (Saavedra et al., 2025)*.

https://doi.org/10.5194/egusphere-2026-2947
Preprint. Discussion started: 12 June 2026

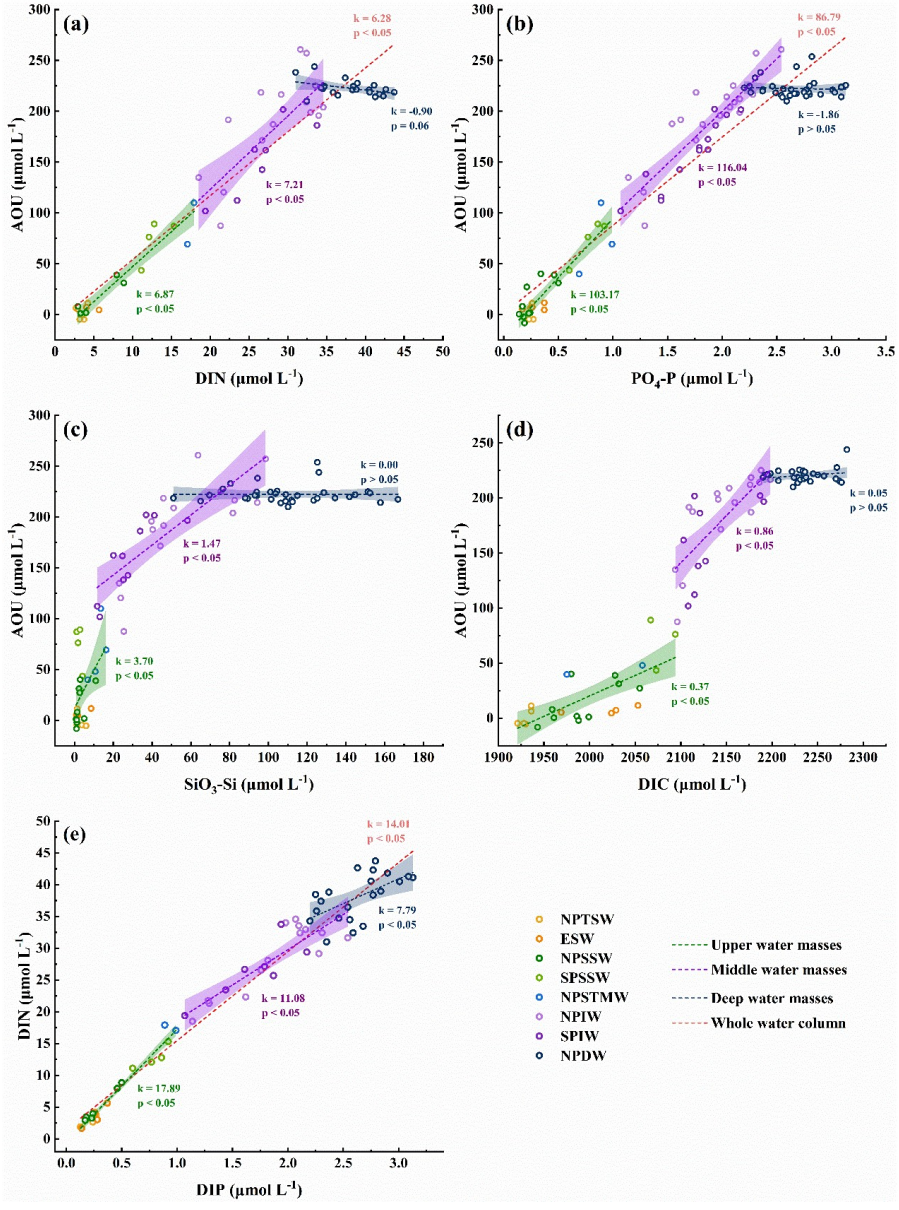

Figure 5. The correlation between apparent oxygen utilization (AOU) and (a) dissolved inorganic nitrogen (DIN), (b) phosphate (PO_4-P, as dissolved inorganic phosphorus, DIP), (c) silicate (SiO_3-Si, as dissolved inorganic silicon, DSi), (d) dissolved inorganic carbon (DIC), and (e) Relationship between DIN and DIP

Unlike DIN and DIP, SiO_3-Si and AOU do not exhibit a clear linear relationship in the whole water column, but instead show distinct vertical stratification. In the upper

https://doi.org/10.5194/egusphere-2026-2947
Preprint. Discussion started: 12 June 2026

waters, intense silicate uptake by phytoplankton such as diatoms drives concentrations to near-zero values (Fig. 5c) (Brzezinski et al., 2024). In the middle waters, the variation in silicate concentration is mainly influenced by diatom deposition and remineralization. As AOU increases, silicates are rapidly released, resulting in an AOU/SiO_3-Si ratio (1.47) lower in these waters than in the upper water masses (3.70) (Figure 5c). In the deep waters, AOU tends to remain nearly constant, whereas SiO_3-Si concentration continued to increase owing to the delayed dissolution of siliceous biogenic debris (Yu et al., 2022). It is estimated that about two-thirds of biogenic silica dissolves at depths shallower than 2,000 m, with the remainder released more slowly at greater depths (Tréguer and De La Rocha, 2013). Consequently, SiO_3-Si levels at depth are largely decoupled from organic matter supply and exhibits no significant linear relationship with AOU (Figure 5c). A similar decoupling between biological consumption and accumulation is observed in the distribution of DIC, which exhibits a characteristic three-stage pattern from surface to deep waters (Fig. 5d). In upper waters, photosynthesis consumes DIC; however, this signal is masked by intense air-sea CO_2 exchange, which leads to a net increase in DIC and consequently a low AOU/DIC ratio of 0.37 (Ito and Reinhard, 2025). In middle waters, organic matter decomposition dominates, and DIC increases rapidly with increasing AOU (AOU/DIC = 0.86, Fig. 5d) (Hu, X et al., 2016). In deep waters, AOU remains stable while DIC accelerates again, due to the accumulation of respired CO_2 from above and enhanced calcium carbonate dissolution with depth (Chen et al., 2022; Feely et al., 2004).

Furthermore, DIN and DIP in each water mass of the study area show a strong linear correlation, and the slope decreases progressively from 17.89 in the upper waters to 11.08 in the middle waters and further to 7.79 in the deep waters, with an overall slope of 14, which is lower than the Redfield ratio (Fig. 5e). The overall low N:P ratio (14) and its vertical decline reflect that phosphorus is regenerated more efficiently than nitrogen in this region. Denitrification, which removes fixed nitrogen, can lower the N:P ratio. However, classical water-column denitrification typically requires dissolved oxygen concentrations below 5 μmol L^{-1} (Deutsch et al., 2011). In the present study, the

https://doi.org/10.5194/egusphere-2026-2947
Preprint. Discussion started: 12 June 2026

minimum observed oxygen concentration exceeds 55 μmol L^{-1}, making extensive pelagic denitrification unlikely. Alternatively, enhanced phosphate release from dissolved organic phosphorus (DOP) via alkaline phosphatase (APase) activity represents one potential mechanism. Although direct APase measurements were not made in this study, previous work has demonstrated that APase produced by Alteromonas can maintain high expression and abundance under phosphorus-limited conditions and even in deeper waters where inorganic phosphorus is not scarce (Saavedra et al., 2025). Given that Alteromonas accounts for a high proportion in all water masses (Fig. 4), it is plausible that this genus contributes to DOP hydrolysis and thereby to the observed low N:P ratio.

4.2 Microbial regulation of non-Redfield stoichiometry in organic matter degradation

The low AOU/DIN (6.28) and AOU/DIP (86.79) ratios observed in the TNWP result from the metabolic strategies of the resident microbial community. Within the study area, *Pelagibacter* and *Alteromonas* emerge as the two most abundant bacterial genera, their complementary metabolic capabilities directly modulate the coupling between organic carbon oxidation and nutrient regeneration, thereby driving the observed deviations from Redfield stoichiometry. *Pelagibacter* exhibits a significant positive correlation with organic matter and a negative correlation with inorganic nutrients (Fig. 6), consistent with its streamlined genome and oligotrophic adaptive strategy (Carini et al., 2013; Giovannoni, 2017). This bacterium lacks the ability to synthesize several essential metabolites and relies on exogenous supply, but its cell surface is enriched with high-affinity transport proteins that enable efficient uptake of small-molecule dissolved organic matter (Giovannoni, 2017). Critically, *Pelagibacter* selectively removes nitrogen-rich organic substrates such as amino acids, proteins, and glucose while leaving behind carbon-rich polymers (Malmstrom et al., 2005).

In contrast, *Alteromonas* displays the opposite environmental correlation pattern: showing a significantly positive correlation with inorganic nutrients and a negative correlation with POC (Fig. 6), reflecting its role as a particle-associated opportunist

https://doi.org/10.5194/egusphere-2026-2947
Preprint. Discussion started: 12 June 2026

with a versatile genome encoding diverse polysaccharide-degrading enzymes (Koch et al., 2019; Lopez-Perez et al., 2012). This genus is a major contributor to alkaline phosphatase gene expression (particularly phoD and phoX) and enzymatic activity (Saavedra et al., 2025). Under phosphorus-limited conditions, these enzymes hydrolyze dissolved organic phosphorus (DOP) to release bioavailable phosphate (Saavedra et al., 2025). *Alteromonas* was abundant in all water masses (Fig. 4), resulting in faster phosphorus regeneration than nitrogen regeneration in the study area, leading to an observed DIN:DIP ratio of approximately 14:1, lower than the Redfield value of 16:1 (Fig. 5e). Beyond these two dominant genera, the ammonia-oxidizing archaeon *Nitrosopumilus*, which is abundant in the subsurface and mid-water (Fig. 4), can mediate high-affinity nitrification and consume oxygen even at extremely low ammonium concentrations (< 10 nmol L^{-1}) (Martens-Habbena et al., 2009).

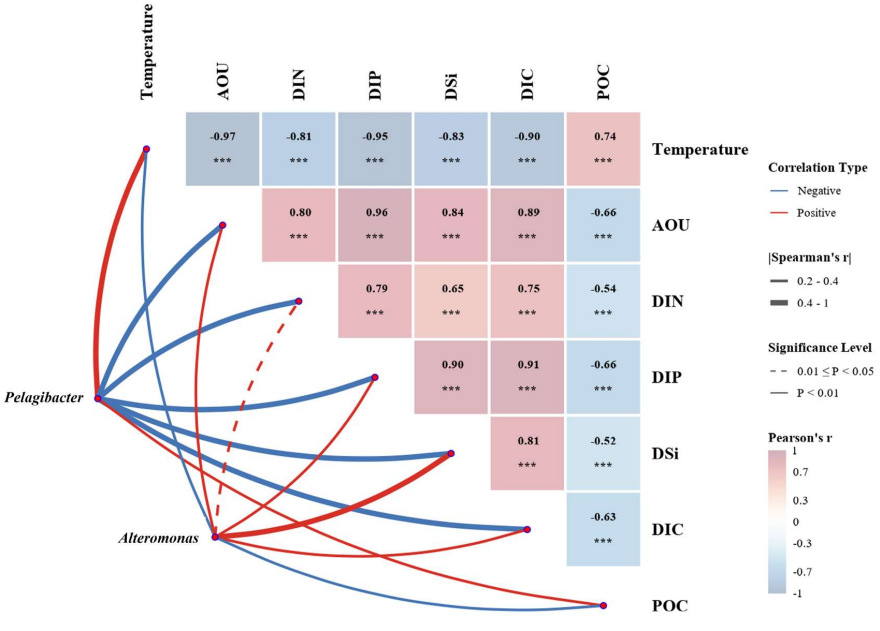

Figure 6. Correlation between dominant microbes and environmental variables. Heatmaps were based on Pearson correlation analysis among environmental variables in the study area (* represents p < 0.01), and Spearman correlation analysis between *Pelagibacter*/*Alteromonas* and environmental variables.**

The ecological division of labor between these functional groups creates a

https://doi.org/10.5194/egusphere-2026-2947
Preprint. Discussion started: 12 June 2026

vertically structured processing network: *Pelagibacter* sustains the microbial loop and small-molecule cycling in oligotrophic surface waters through high-affinity uptake, while *Alteromonas* dominates the degradation of settling TEP and other complex polymers, releasing inorganic nutrients in deeper waters (Robertson et al., 2024). This functional differentiation enables the preferential degradation of low C:N substrates, coupled with active phosphorus scavenging from organic pools, driving the system toward enhanced nutrient regeneration relative to organic carbon oxidation, thereby maintaining a dynamic equilibrium in its biogeochemical cycles and overall ecosystem function.

4.3 Coupled physical-biogeochemical-microbial controls on carbon and nutrient cycling in the TNWP

The strong vertical stratification of the TNWP creates a multi-water-mass structure. Nutrients are primarily retained in deep reservoirs and remain chronically depleted in surface waters. Nutrient regeneration in subsurface waters relies mainly on the release during organic matter degradation (Hirose and Kamiya, 2003). In this nutrient-poor surface environment, large amounts of TEP with a high C: N ratio accumulate (Fig. 3i). The synthesis of this carbon-rich organic matter creates an imbalance between oxygen production and nitrate consumption, leading to positive anomalies in the $PrePO_4$ and $PreNO_3$ in surface waters (Figs. 3 d, e) (Curran et al., 2025). POM is gradually degraded during settling, while intermediate and deep waters are active areas for heterotrophic respiration. It is estimated that approximately 90 % of the organic matter exported to this area is remineralized and releases CO_2 (Robinson et al., 2010). This process consumes a large amount of DO, and the strong stratification hinders the timely replenishment of DO in the intermediate and deep waters, thereby forming low oxygen zones in these water masses (Fig. 7).

https://doi.org/10.5194/egusphere-2026-2947
Preprint. Discussion started: 12 June 2026

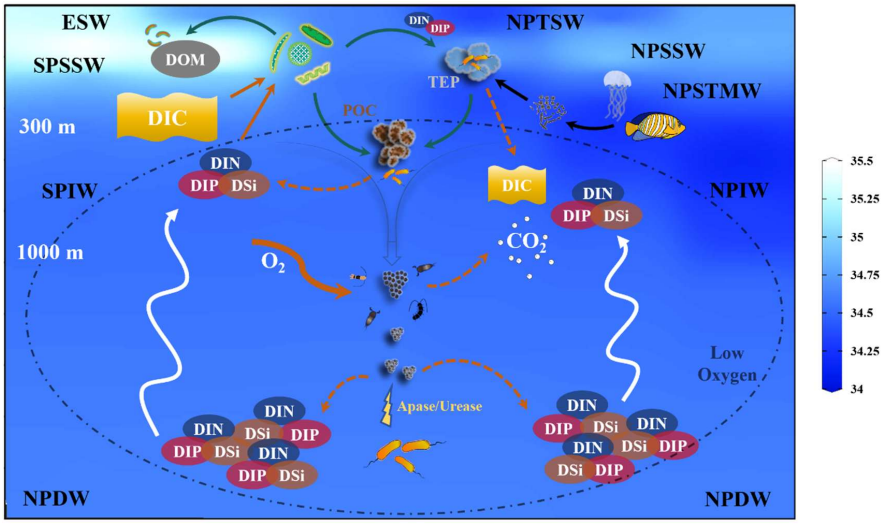

Figure 7. Schematic diagram of coupled physical-biogeochemical-microbial controls on carbon and nutrient cycling in the study area with a salinity background.

Simultaneously, nutrient release also mainly occurs in the intermediate and deep water masses, exhibiting a clear regeneration gradient from shallow to deep (Figs. 3a-c) (Hirose and Kamiya, 2003). The distribution patterns and functional traits of key bacteria in the water column are closely linked to their distinct ecological niches. *Pelagibacter* is abundant in oligotrophic surface waters (Fig. 4), and its streamlined genome and metabolic mechanisms enable it to drive the remineralization of small-molecule organic carbon and nutrient recycling through slow but continuous growth (Sun, J et al., 2011). *Alteromonas* relies on a diverse enzyme system to efficiently respond to organic substrates, thereby utilizing complex polymers (Koch et al., 2019). This functional differentiation within the microbial community maintains the slow cycling of dissolved organic matter under oligotrophic conditions and ensures the efficient degradation of complex polymeric organic matter when available, thereby regulating both the pathways and the intensity of carbon, nitrogen, and phosphorus cycling in the water column.

5. Conclusions

The oligotrophic waters of the tropical Northwest Pacific are characterized by

https://doi.org/10.5194/egusphere-2026-2947
Preprint. Discussion started: 12 June 2026

pronounced vertical stratification, with nutrients largely trapped at depth, while surface waters remain chronically nutrient-poor. Phytoplankton adapt to chronic nutrient stress by producing carbon-rich transparent exopolymer particles, whereas the microbial community exhibits functional partitioning, in which oligotrophic *Pelagibacter* recycles small organic molecules, and opportunistic *Alteromonas* degrades polymers, releasing phosphorus through alkaline phosphatase activity. This selective processing enhances nutrient regeneration relative to carbon oxidation, depresses DIN:DIP ratios throughout the water column, and generates the observed low AOU/DIN (6.28) and AOU/DIP (86.79) ratios. Collectively, our findings establish that organism-level adaptations to nutrient stress can fundamentally restructure the stoichiometry of organic matter degradation in oligotrophic oceans. This biologically mediated stoichiometric imbalance challenges the core assumption of invariant Redfield ratios embedded in current biogeochemical models, suggesting that incorporating such microbial-driven flexibility in carbon-nitrogen-phosphorus coupling is essential for improving predictions of carbon export efficiency and ocean carbon storage under future climate scenarios.

Data Availability: The data used in this paper are available at Figshare (*Tian,* 2026).

Competing interests: The authors declare that they have no conflict of interest.

Author contributions: Detong Tian carried out the investigation, developed the methodology, performed data curation and visualization, and prepared the original draft. Xuegang Li and Yunping Xu acquired the funding, and reviewed and edited the manuscript. Feng Zhao provided resources. Jun Ma, Shanshan Liu, and Muhammad Inayat Ullah Khan reviewed and edited the manuscript. Weichao Wu conceptualized the study, and reviewed and edited the manuscript.

Acknowledgments: We appreciate the crews of the R/V *Kexue* for sampling assistance during the cruise of NORC2021-09 supported by the National Natural Science Foundation of China (project no. 42049909).

Financial support: This work was supported by the key program of National Natural

https://doi.org/10.5194/egusphere-2026-2947
Preprint. Discussion started: 12 June 2026

Science Foundation of China (Grant No. 42530401) and the National Natural Science Foundation of China (Grant No. 42476204).

References

Álvarez-Salgado, X. A., Álvarez, M., Brea, S., Mèmery, L.,Messias, M. J.: Mineralization of biogenic materials in the water masses of the South Atlantic Ocean. II: Stoichiometric ratios and mineralization rates, Prog. Oceanogr., *123*, 24-37, https://doi.org/10.1016/j.pocean.2013.12.009, 2014.

Anderson, L. A.,Sarmiento, J. L.: Redfield ratios of remineralization determined by nutrient data analysis, Global. Biogeochem. Cycles., *8*(1), 65-80, https://doi.org/10.1029/93gb03318, 1994.

Bittar, T. B., Passow, U., Hamaraty, L., Bidle, K. D.,Harvey, E. L.: An updated method for the calibration of transparent exopolymer particle measurements, Limnol. Oceanogr. Methods., *16*(10), 621-628, https://doi.org/10.1002/lom3.10268, 2018.

Bryan, J. R., Rlley, J. P.,Williams, P. J. L.: A winkler procedure for making precise measurements of oxygen concentration for productivity and related studies, J. Exp. Mar. Bio. Ecol., *21*(3), 191-197, https://doi.org/10.1016/0022-0981(76)90114-3, 1976.

Brzezinski, M. A., Johnson, L., Estapa, M., Clevenger, S., Roca-Martí, M., Romanelli, E., et al.: Physical Mechanisms Sustaining Silica Production Following the Demise of the Diatom Phase of the North Atlantic Spring Phytoplankton Bloom During EXPORTS, Global. Biogeochem. Cycles., *38*(7), e2023GB008048, https://doi.org/10.1029/2023gb008048, 2024.

Calleja, M. L., Al-Otaibi, N.,Moran, X. A. G.: Dissolved organic carbon contribution to oxygen respiration in the central Red Sea, Sci. Rep., *9*(1), 4690, https://doi.org/10.1038/s41598-019-40753-w, 2019.

Carini, P., Steindler, L., Beszteri, S.,Giovannoni, S. J.: Nutrient requirements for growth of the extreme oligotroph 'Candidatus Pelagibacter ubique' HTCC1062 on a defined medium, ISME J., *7*(3), 592-602, https://doi.org/10.1038/ismej.2012.122, 2013.

Chen, H., Haumann, F. A., Talley, L. D., Johnson, K. S.,Sarmiento, J. L.: The Deep Oceans Carbon Exhaust, Global. Biogeochem. Cycles., *36*(7), e2021GB007156, https://doi.org/10.1029/2021GB007156, 2022.

Curran, K., Villareal, T. A.,Letscher, R. T.: A time series analysis of transparent exopolymer particle distributions and C : N stoichiometry in the subtropical North Pacific: a key process in net community production and preformed nitrate anomalies?, Biogeosciences., *22*(14), 3515-3531, https://doi.org/10.5194/bg-22-3515-2025, 2025.

Dai, M., Luo, Y. W., Achterberg, E. P., Browning, T. J., Cai, Y., Cao, Z., et al.: Upper Ocean Biogeochemistry of the Oligotrophic North Pacific Subtropical Gyre: From Nutrient Sources to Carbon Export, Rev. Geophys., *61*(3), e2022RG000800, https://doi.org/10.1029/2022rg000800, 2023.

Delaigue, L., Sulpis, O., Reichart, G. J.,Humphreys, M. P.: The Changing Biological Carbon Pump of the South Atlantic Ocean, Global. Biogeochem. Cycles., *38*(9), e2024GB008202, https://doi.org/10.1029/2024gb008202, 2024.

Deutsch, C., Brix, H., Ito, T., Frenzel, H.,Thompson, L.: Climate-forced variability of ocean hypoxia, Science., *333*(6040), 336-339, https://doi.org/10.1126/science.1202422, 2011.

Digernes, M. G., Bodur, Y. V., Amargant-Arumí, M., Müller, O., Hawkes, J. A., Kohler, S. G., et al.:

https://doi.org/10.5194/egusphere-2026-2947
Preprint. Discussion started: 12 June 2026

Contrasting seasonal patterns in particle aggregation and dissolved organic matter transformation in a sub-Arctic fjord, Biogeosciences., *22*(2), 601-623, https://doi.org/10.5194/bg-22-601-2025, 2025.

Engel, A.,Passow, U.: Carbon and nitrogen content of transparent exopolymer particles (TEP) in relation to their Alcian Blue adsorption, Mar. Ecol. Prog. Ser., *219*, 1-10, https://doi.org/10.3354/meps219001, 2001.

Feely, R. A., Sabine, C. L., Lee, K., Berelson, W., Kleypas, J., Fabry, V. J., et al.: Impact of anthropogenic CO_2 on the $CaCO_3$ system in the oceans, Science., *305*(5682), 362-366, https://doi.org/10.1126/science.1097329, 2004.

Friedlingstein, P., O'Sullivan, M., Jones, M. W., Andrew, R. M., Hauck, J., Landschützer, P., et al.: Global Carbon Budget 2024, Earth. Syst. Sci. Data., *17*(3), 965-1039, https://doi.org/10.5194/essd-17-965-2025, 2025.

Garcia, H. E.,Gordon, L. I.: Oxygen solubility in seawater: Better fitting equations, Limnol. Oceanogr., *37*(6), 1307-1312, https://doi.org/10.4319/lo.1992.37.6.1307, 1992.

Giovannoni, S. J.: SAR11 Bacteria: The Most Abundant Plankton in the Oceans, Ann. Rev. Mar. Sci., *9*, 231-255, https://doi.org/10.1146/annurev-marine-010814-015934, 2017.

Guo, J., Zhou, B., Achterberg, E. P., Yuan, H., Song, J., Duan, L., et al.: Rapid Cycling of Bacterial Particulate Organic Matter in the Upper Layer of the Western Pacific Warm Pool, Geophys. Res. Lett., *50*(11), e2023GL102896, https://doi.org/10.1029/2023gl102896, 2023.

Hirose, K.,Kamiya, H.: Vertical Nutrient Distributions in the Western North Pacific Ocean: Simple Model for Estimating Nutrient Upwelling, Export Flux and Consumption Rates, J. Oceanogr., *59*(2), 149-161, https://doi.org/10.1023/a:1025535003841, 2003.

Hu, D., Wu, L., Cai, W., Gupta, A. S., Ganachaud, A., Qiu, B., et al.: Pacific western boundary currents and their roles in climate, Nature., *522*(7556), 299-308, https://doi.org/10.1038/nature14504, 2015.

Hu, X., Cai, W.-J., Rabalais, N. N.,Xue, J.: Coupled oxygen and dissolved inorganic carbon dynamics in coastal ocean and its use as a potential indicator for detecting water column oil degradation, Deep-Sea Res. Part. II. Top. Stud. Oceanogr., *129*, 311-318, https://doi.org/10.1016/j.dsr2.2014.01.010, 2016.

Hwang, J., Druffel, E. R. M., Eglinton, T. I.,Repeta, D. J.: Source(s) and cycling of the nonhydrolyzable organic fraction of oceanic particles, Geochim. Cosmochim. Acta. *70*(20), 5162-5168, https://doi.org/10.1016/j.gca.2006.07.020, 2006.

Ito, T., Follows, M. J.,Boyle, E. A.: Is AOU a good measure of respiration in the oceans?, Geophys. Res. Lett., *31*(17), L17305, https://doi.org/10.1029/2004gl020900, 2004.

Ito, T.,Reinhard, C. T.: A New Framework for the Attribution of Air-Sea CO_2 Exchange, Global. Biogeochem. Cycles., *39*(2), e2024GB008346, https://doi.org/10.1029/2024gb008346, 2025.

Jian, Z., Wang, Y., Dang, H., Mohtadi, M., Rosenthal, Y., Lea, D. W., et al.: Warm pool ocean heat content regulates ocean-continent moisture transport, Nature., *612*(7938), 92-99, https://doi.org/10.1038/s41586-022-05302-y, 2022.

Kharbush, J. J., Close, H. G., Van Mooy, B. A. S., Arnosti, C., Smittenberg, R. H., Le Moigne, F. A. C., et al.: Particulate Organic Carbon Deconstructed: Molecular and Chemical Composition of Particulate Organic Carbon in the Ocean, Front. Mar. Sci. *7*, 518, https://doi.org/10.3389/fmars.2020.00518, 2020.

Koch, H., Freese, H. M., Hahnke, R. L., Simon, M.,Wietz, M.: Adaptations of Alteromonas sp. 76-1 to Polysaccharide Degradation: A CAZyme Plasmid for Ulvan Degradation and Two Alginolytic Systems, Front. Microbiol., *10*, 504, https://doi.org/10.3389/fmicb.2019.00504, 2019.

https://doi.org/10.5194/egusphere-2026-2947
Preprint. Discussion started: 12 June 2026

637 Kodama, T., Kurogi, H., Okazaki, M., Jinbo, T., Chow, S., Tomoda, T., et al.: Vertical distribution of
638 transparent exopolymer particle (TEP) concentration in the oligotrophic western tropical North
639 Pacific, Mar. Ecol. Prog. Ser., *513*, 29-37, https://doi.org/10.3354/meps10954, 2014.
640 Körtzinger, A., Hedges, J. I.,Quay, P. D.: Redfield ratios revisited: Removing the biasing effect of
641 anthropogenic CO_2, Limnol. Oceanogr., *46*(4), 964-970, https://doi.org/10.4319/lo.2001.46.4.0964,
642 2001.
643 Letscher, R. T.,Villareal, T. A.: Evaluation of the seasonal formation of subsurface negative preformed
644 nitrate anomalies in the subtropical North Pacific and North Atlantic, Biogeosciences., *15*(21),
645 6461-6480, https://doi.org/10.5194/bg-15-6461-2018, 2018.
646 Liu, W., Zhao, F., Li, X., Zheng, S., Li, L., Zhao, R., et al.: Enhanced nutrient supply promotes mutualistic
647 interactions between cyanobacteria and bacteria in oligotrophic ocean, Proc. R. Soc. B. Biol. Sci.,
648 *291*(2027), 20240788, https://doi.org/10.1098/rspb.2024.0788, 2024.
649 Longhurst, A. R.,Glen Harrison, W.: The biological pump: Profiles of plankton production and
650 consumption in the upper ocean, Prog. Oceanogr., *22*(1), 47-123, https://doi.org/10.1016/0079-
651 6611(89)90010-4, 1989.
652 Lopez-Perez, M., Gonzaga, A., Martin-Cuadrado, A. B., Onyshchenko, O., Ghavidel, A., Ghai, R., et al.:
653 Genomes of surface isolates of Alteromonas macleodii: the life of a widespread marine
654 opportunistic copiotroph, Sci. Rep., *2*, 696, https://doi.org/10.1038/srep00696, 2012.
655 Ma, J., Song, J., Li, X., Wang, Q., Yuan, H., Li, N., et al.: Analysis of differences in nutrients chemistry
656 in seamount seawaters in the Kocebu and M4 seamounts in Western Pacific Ocean, J. Oceanol.
657 Limnol., *39*(5), 1662-1674, https://doi.org/10.1007/s00343-020-0239-7, 2021a.
658 Ma, J., Song, J., Li, X., Wang, Q., Zhong, G., Yuan, H., et al.: The OMZ and Its Influence on POC in the
659 Tropical Western Pacific Ocean: Based on the Survey in March 2018, Front. Earth Sci., *9*, 632229,
660 https://doi.org/10.3389/feart.2021.632229, 2021b.
661 Ma, J., Song, J., Li, X., Yuan, H., Li, N., Duan, L., et al.: Control factors of DIC in the Y3 seamount
662 waters of the Western Pacific Ocean, J. Oceanol. Limnol., *38*(4), 1215-1224,
663 https://doi.org/10.1007/s00343-020-9314-3, 2020.
664 Malmstrom, R. R., Cottrell, M. T., Elifantz, H.,Kirchman, D. L.: Biomass production and assimilation of
665 dissolved organic matter by SAR11 bacteria in the Northwest Atlantic Ocean, Appl. Environ.
666 Microbiol., *71*(6), 2979-2986, https://doi.org/10.1128/AEM.71.6.2979-2986.2005, 2005.
667 Martens-Habbena, W., Berube, P. M., Urakawa, H., de la Torre, J. R.,Stahl, D. A.: Ammonia oxidation
668 kinetics determine niche separation of nitrifying Archaea and Bacteria, Nature., *461*(7266), 976-
669 979, https://doi.org/10.1038/nature08465, 2009.
670 Radenac, M.-H., Messié, M., Léger, F.,Bosc, C.: A very oligotrophic zone observed from space in the
671 equatorial Pacific warm pool, Remote Sens. Environ., *134*, 224-233,
672 https://doi.org/10.1016/j.rse.2013.03.007, 2013.
673 Redfield, A. C.: The biological control of chemical factors in the environment, Sci. Prog., *11*, 150-170,
674 1960.
675 Robertson, J. M., Garza, E. A., Stubbusch, A. K. M., Dupont, C. L., Hwa, T.,Held, N. A.: Marine bacteria
676 Alteromonas spp. require UDP-glucose-4-epimerase for aggregation and production of sticky
677 exopolymer, mBio., *15*(8), e0003824, https://doi.org/10.1128/mbio.00038-24, 2024.
678 Robinson, C., Steinberg, D. K., Anderson, T. R., Arístegui, J., Carlson, C. A., Frost, J. R., et al.:
679 Mesopelagic zone ecology and biogeochemistry – a synthesis, Deep-Sea Res. Part. II. Top. Stud.
680 Oceanogr., *57*(16), 1504-1518, https://doi.org/10.1016/j.dsr2.2010.02.018, 2010.

https://doi.org/10.5194/egusphere-2026-2947
Preprint. Discussion started: 12 June 2026

Saavedra, D. E. M., Gonzalez, J. M., Klaushofer, K., Breyer, E., Afjehi-Sadat, L., Bulgheresi, S., et al.: Multifunctionally diverse alkaline phosphatases of Alteromonas drive the phosphorus cycle in the ocean, Nat. Commun., *16*(1), 9789, https://doi.org/10.1038/s41467-025-64455-2, 2025.

Singh, A., Baer, S. E., Riebesell, U., Martiny, A. C.,Lomas, M. W.: C : N : P stoichiometry at the Bermuda Atlantic Time-series Study station in the North Atlantic Ocean, Biogeosciences., *12*(21), 6389-6403, https://doi.org/10.5194/bg-12-6389-2015, 2015.

Smith, C. R., De Leo, F. C., Bernardino, A. F., Sweetman, A. K.,Arbizu, P. M.: Abyssal food limitation, ecosystem structure and climate change, Trends Ecol. Evol., *23*(9), 518-528, https://doi.org/10.1016/j.tree.2008.05.002, 2008.

Smyth, A. J.,Letscher, R. T.: Spatial and temporal occurrence of preformed nitrate anomalies in the subtropical North Pacific and North Atlantic oceans, Mar. Chem., *252*, 104248, https://doi.org/10.1016/j.marchem.2023.104248, 2023.

Sulpis, O., Trossman, D. S., Holzer, M., Jeansson, E., Lauvset, S. K.,Middelburg, J. J.: Respiration Patterns in the Dark Ocean, Global. Biogeochem. Cycles., *37*(8), e2023GB007747, https://doi.org/10.1029/2023gb007747, 2023.

Sun, C., Xu, J., Liu, Z., Tong, M.,Zhu, B.: Application of Argo Data in the Analysis of Water Masses in the Northwest Pacific Ocean, Mar. Sci. Bull., *10*, 1-13, 2008.

Sun, J., Steindler, L., Thrash, J. C., Halsey, K. H., Smith, D. P., Carter, A. E., et al.: One carbon metabolism in SAR11 pelagic marine bacteria, PLoS One., *6*(8), e23973, https://doi.org/10.1371/journal.pone.0023973, 2011.

Tanioka, T.,Matsumoto, K.: Stability of Marine Organic Matter Respiration Stoichiometry, Geophys. Res. Lett., *47*(1), e2019GL085564, https://doi.org/10.1029/2019gl085564, 2020.

Tian, D., Li, X., Song, J., Ma, J., Yuan, H.,Duan, L.: Biogeochemical layering and transformation of particulate organic carbon in the Tropical Northwestern Pacific Ocean inferred from $\delta^{13}C$, Ocean Sci., *21*(4), 1627-1639, https://doi.org/10.5194/os-21-1627-2025, 2025.

Tian, D.: Stoichiometric deviation and regulatory mechanisms of organic matter degradation in oligotrophic ocean of the Northwest Pacific, Figshare [data set], https://doi.org/10.6084/m9.figshare.31841125, 2026.

Tréguer, P. J.,De La Rocha, C. L.: The world ocean silica cycle, Ann. Rev. Mar. Sci., *5*, 477-501, https://doi.org/10.1146/annurev-marine-121211-172346, 2013.

Yamada, Y., Yokokawa, T., Uchimiya, M., Nishino, S., Fukuda, H., Ogawa, H., et al.: Transparent exopolymer particles (TEP) in the deep ocean: full-depth distribution patterns and contribution to the organic carbon pool, Mar. Ecol. Prog. Ser., *583*, 81-93, https://doi.org/10.3354/meps12339, 2017.

Yu, X., Zhuang, Y., Cai, X.,Qi, D.: Role of Marginal Seas in Deep Ocean Regeneration of Dissolved Silica: A Case Study in the Marginal Seas of the Western Pacific, Front. Mar. Sci. *9*, 925919, https://doi.org/10.3389/fmars.2022.925919, 2022.

Zamanillo, M., Ortega-Retuerta, E., Nunes, S., Rodríguez-Ros, P., Dall'Osto, M., Estrada, M., et al.: Main drivers of transparent exopolymer particle distribution across the surface Atlantic Ocean, Biogeosciences., *16*(3), 733-749, https://doi.org/10.5194/bg-16-733-2019, 2019.

Zhu, Z., Song, G., Zhang, Z., Luo, Y., Liu, S.,Zhang, J.: On the Stoichiometry of Degradable Fraction of Particulate Organic Matter Along a Diapycnal Mixing Path Using Dissolved Oxygen $\delta^{18}O$ Approach, J. Geophys. Res. Oceans., *130*(6), e2025JC022512, https://doi.org/10.1029/2025jc022512, 2025.